풍하중을 받는 평면 막구조물의 동적불안정 판정에 관한 연구

Study on Dynamic Instability of Plane Membrane Structures under Wind Action

한 상 을† 후 효 무*
Han, Sung-Eul Hou, Xiao-Wu
(논문접수일 : 2008년 11월 17일 ; 심사종료일 : 2009년 4월 2일)

요 지

본 논문에서는 풍하중을 받는 평면 막구조물의 동적불안정 판정을 규명하였다. 풍하중을 받는 막구조물의 지배방정식을 정식화할 경우 가장 중요한 것은 막 표면의 공기 압력을 합리적으로 산정하는 것이다. 베르누이 원리에 의하여 유체 압력은 속도 퍼텐셜과 관계를 가지며 얇은 날개 원리에 의해 막 표면 공기의 움직임을 일련의 와류로 간주하고 속도 퍼텐셜을 구할 수 있다. 이 논문에서는 가장 많이 쓰이는 3 절점 삼각형 막요소를 이용하여 가중 잔여치 갤러킨법을 적용한 안정 평가의 판별식을 유도하였다. 수치해석 모델로는 정사각형과 직사각형의 막구조물을 채택하였고 임계 풍속에 대한 초기인장력과 풍방향의 영향을 분석하였다.

핵심용어 : 동적불안정, 플러터, 풍하중, 막구조물, 얇은 날개 이론

Abstract

In this paper, dynamic instability of plane membrane structures under wind action has been studied. The key to solving the governing equations of membrane structures under wind action is how to obtain the air pressure on membrane. Based on Bernoulli's theorem, fluid pressure has a certain relationship with velocity potential. Velocity potential could be solved according to thin aerofoil theory, where air around the membrane is regarded as a sheet of vortices. In this paper, we take advantage of the most commonly used three-node triangular membrane element and weighted residual-Galerkin method to obtain the determining equation for stability evaluation. Square and rectangular membrane structures are studied. The influence of initial prestressing force and wind direction towards critical wind velocity are also analyzed in this paper.

Keywords *: dynamic instability, flutter, wind action, membrane structures, thin aerofoil theory*

1. 서 론

As a newly developed structural system, membrane structure attracts more and more attention due to its advantages such as light weight, easily constructed, good aseismatic and economic property and so on. It is widely applied in stadium, airport and other large spatial structural systems.

Because membrane structures are light weighted and flexible, they possess a good earthquake resistant property. However, they are highly susceptible to the wind action simultaneously. Based on these properties, wind load is regarded as the dominant load in dynamic analysis of membrane structures. When wind velocity reaches a certain value, loss of stability may occur, which contains "divergence type" and "flutter type". Divergence type instability means that structure moves with exponentially growing displacement and without vibration. On the contrary, flutter type instability means that structure vibrates with exponentially growing amplitude.

This kind of aeroelastic instability was firstly

† 책임저자, 정회원 · 인하대학교 건축학부 교수
Tel: 032-873-5724 ; Fax: 032-873-5724
E-mail: hsang@inha.ac.kr
* 인하대학교 건축공학과 박사과정

• 이 논문에 대한 토론을 2009년 6월 30일까지 본 학회에 보내주시면 2009년 8월호에 그 결과를 게재하겠습니다.

studied in aerospace field. The results were further applied into studies of bridge, plate and shell as well as membrane structures. Among the papers obtained, Kunieda (1975) firstly presented the method to determine flutter critical wind velocity of hanging membrane roofs. After that, Kornecki(1976), Newman and Paidoussis(1991), Lucey and Carpenter(1992) all try to make use of analytical method to solve this kind of instability problem. Sygulski(1993; 1996; 1997; 2007) is the first person to take advantage of numerical method to solve aeroelastic instability.

In this paper, we will introduce how to use FEA method to solve aeroelastic instability of membrane structures. In chapter 2, we will introduce some basic formulations. Among them, the most important thing is to obtain air pressure on membrane. In this paper, we will solve air pressure on membrane based on "thin aerofoil theory". In chapter 3, we will interpret how to use FEA method to solve these basic formulations. In chapter 4, stability criteria will be introduced. Whether the membrane structure is unstable will be determined according to these criteria. Finally, two numerical examples will be studied in chapter 5, which include square and rectangular membrane structures. The impact of prestressing force and wind direction will be analyzed.

2. Basic formulation

The governing equation of motion for membrane structure under wind action is

$$T_x \frac{\partial^2 w}{\partial x^2} + T_y \frac{\partial^2 w}{\partial y^2} - \rho_s \frac{\partial^2 w}{\partial t^2} + \Delta p = 0 \tag{1}$$

Where,

T_x, T_y - prestressing forces in x and y direction

ρ_s - density of membrane

w - displacement in z direction

$\Delta p = p_1 - p_2$, pressure difference

p_1, p_2 - air pressure on the upper and lower side of membrane

Pressure on each side could be obtained from Bernoulli's equation.

$$p = -\rho_a \left(\frac{\partial \phi}{\partial t} + U \frac{\partial \phi}{\partial x_\alpha} \right) \tag{2}$$

Where, ρ_a - density of air

ϕ - disturbance velocity potential

U - wind velocity

α - wind direction angle

Velocity potential should satisfy Laplace's equation.

$$\nabla^2 \phi = 0 \tag{3}$$

The solution of Eq. (3) for the half space ($z \geq 0$) of the incompressible air could be expressed based on thin aerofoil theory.

$$\phi(p,t) = \frac{1}{2\pi} \int_S \frac{\partial \phi}{\partial z} \cdot \frac{1}{r(P,Q)} dS_Q = \frac{1}{2\pi} \int_S f \cdot \frac{1}{r(P,Q)} dS_Q \tag{4}$$

$f = \frac{\partial \phi}{\partial z}$ - disturbance velocity in z direction

$r(P,Q)$ - distance between point $\boldsymbol{P}$ and $\boldsymbol{Q}$, $\boldsymbol{P}$ and $\boldsymbol{Q}$ are arbitrary points on the surface.

Apart from that, disturbance velocity and the motion of membrane should satisfy following relationship.

$$f = \frac{\partial \phi}{\partial z} = \frac{\partial w}{\partial t} + U \frac{\partial w}{\partial x_\alpha} \tag{5}$$

3. Numerical method by FEA

Separating the variables into time term and space term, for example, $\phi(P,t) = \tilde{\phi}(x,y) \cdot T(t)$ and expressing the time term with the exponential form: $T(t) = e^{\lambda t}$, then $\phi(P,t) = \tilde{\phi}(x,y) \cdot e^{\lambda t}$. Thus, Eqs. (1), (2), (4), (5) could be transformed as follows:

$$T_x \frac{\partial^2 \tilde{w}}{\partial x^2} + T_y \frac{\partial^2 \tilde{w}}{\partial y^2} - \lambda^2 \rho_s \tilde{w} + \Delta \tilde{p} = 0 \tag{6}$$

$$\tilde{p} = -\rho_a \left(\lambda \tilde{\phi} + U \frac{\partial \tilde{\phi}}{\partial x_\alpha} \right) \tag{7}$$

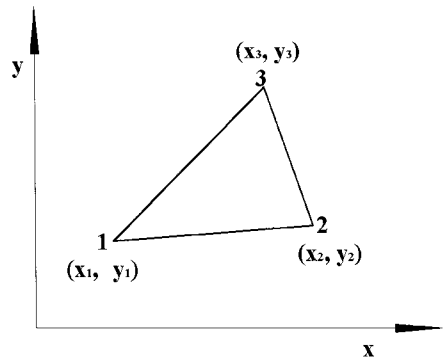

Fig. 1 Three-node triangular element

$$\tilde{\phi} = \frac{1}{2\pi}\int_S \tilde{f}\cdot\frac{1}{r(P,Q)}dS_Q \tag{8}$$

$$\tilde{f} = \lambda\tilde{w} + U\frac{\partial\tilde{w}}{\partial x_\alpha} \tag{9}$$

The most commonly used three-node triangular element (as shown in Fig. 1) will be used to solve above four equations. Before calculation, we should define shape functions firstly.

Shape functions could be defined with the coordinates of three end nodes.

$$N_1 = \frac{1}{2\Delta}\left[(x_2y_3 - x_3y_2) + (y_2 - y_3)x + (x_3 - x_2)y\right] \tag{10a}$$

$$N_2 = \frac{1}{2\Delta}\left[(x_3y_1 - x_1y_3) + (y_3 - y_1)x + (x_1 - x_3)y\right] \tag{10b}$$

$$N_3 = \frac{1}{2\Delta}\left[(x_1y_2 - x_2y_1) + (y_1 - y_2)x + (x_2 - x_1)y\right] \tag{10c}$$

Where, $\Delta = \frac{1}{2}\det\begin{vmatrix}1 & x_1 & y_1\\ 1 & x_2 & y_2\\ 1 & x_3 & y_3\end{vmatrix}$ (area of triangle)

Here, x and y are coordinates of an arbitrary point inside the triangle. With these shape functions, any variables of a point inside the triangle could be expressed by its three end points. For example, the disturbance velocity potential of a point is

$$\tilde{\phi}(x,y) = \begin{bmatrix}N_1 & N_2 & N_3\end{bmatrix}\begin{Bmatrix}\bar{\phi}_1\\ \bar{\phi}_2\\ \bar{\phi}_3\end{Bmatrix} = [N]\{\bar{\phi}\} \tag{11}$$

According to the weighted residual-Galerkin method, Eqs. (6), (7), (8), (9) could be solved by approximating them in an integral form over an element, where the shape functions are used as weighting functions. Take Eq. (9) for example,

$$\int_\Omega N^T\left(\tilde{f} - \lambda\tilde{w} - U\frac{\partial\tilde{w}}{\partial x_\alpha}\right)\,d\Omega = 0 \tag{12}$$

Where, $\tilde{f}$, $\tilde{w}$, $\frac{\partial\tilde{w}}{\partial x_\alpha}$ could be expressed by end point value through shape functions.

$$\tilde{f} = [N]\{\bar{f}\} \tag{13a}$$

$$\tilde{w} = [N]\{\bar{w}\} \tag{13b}$$

$$\frac{\partial\tilde{w}}{\partial x_\alpha} = \left[\frac{\partial N}{\partial x_\alpha}\right]\{\bar{w}\} \tag{13c}$$

Then Eq. (12) could be transformed as follows.

$$B_1\bar{f} = \lambda B_1\bar{w} + UB_2\bar{w} \tag{14}$$

For the same reason, Eqs. (15), (16) and (17) could be obtained.

$$T_xB_3 + T_yB_4 - \lambda^2\rho_sB_1\bar{w} + \Delta\bar{p} = 0 \tag{15}$$

$$B_1\bar{p} = -\rho_a(\lambda B_1 + UB_2)\bar{\phi} \tag{16}$$

$$\bar{\phi} = B_5\bar{f} \tag{17}$$

Here,

$$B_1^i = \int_{\Omega_i} N^T\cdot N\;\;d\Omega \tag{18a}$$

$$B_2^i = \int_{\Omega_i} N^T\cdot\frac{\partial N}{\partial x_\alpha}d\Omega \tag{18b}$$

$$B_3^i = -\int_{\Omega_i}\frac{\partial N^T}{\partial x}\cdot\frac{\partial N}{\partial x}d\Omega \tag{18c}$$

$$B_4^i = -\int_{\Omega_i}\frac{\partial N^T}{\partial y}\cdot\frac{\partial N}{\partial y}d\Omega \tag{18d}$$

(i is the number of element)

B_5 in Eq. (17) could be obtained as follows.

$$B_5(P,K) = \frac{1}{2\pi}\sum_{i=1}^{n_e}\int_{\Omega_i}\frac{N_j(x,y)}{r(P,Q)}d\Omega \tag{19}$$

Where, n_e - number of element relevant to point K.

$N_j(x,y)$ - shape function of point $Q(x,y)$. j=1 or 2

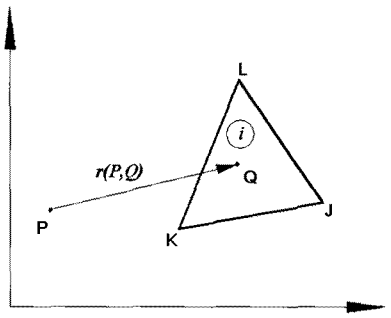

Fig. 2 Variables used in Eq. (19).

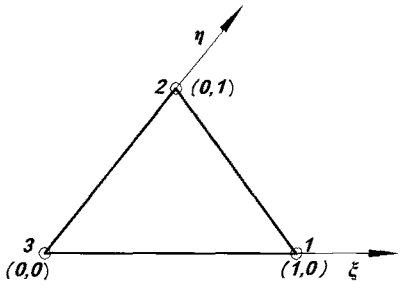

Fig. 3 Triangular coordinates

or 3, which depends on the definition of element I.

Numerical integration over a triangle as Eq. (19) could be performed in terms of the triangular coordinates(Fig. 3) through coordinates transformation.

$$\int_S f(x,y)dS = \int_0^1 \int_0^{1-\xi} f(\xi,\eta)\cdot J(\xi,\eta)\ d\eta\ d\xi = \sum_{i=1}^{n} f(\xi_i,\eta_i)\cdot J(\xi_i,\eta_i)\cdot w_i \quad (20)$$

Where, $J(\xi,\eta)$ - Jacobian matrix. $J=\begin{vmatrix} \frac{\partial x}{\partial \xi} & \frac{\partial y}{\partial \xi} \\ \frac{\partial x}{\partial \eta} & \frac{\partial y}{\partial \eta} \end{vmatrix}$

n - number of Gauss integration points

w_i - weighting factor

Substituting Eq. (14), (16), (17) into Eq. (15), we could obtain final Eq. (21).

$$(K+\lambda D+\lambda^2 M)\overline{w}=0 \quad (21)$$

Where, $K = K_s + K_a$

$K_s = T_x B_3 + T_y B_4$ (structural stiffness)

$K_a = \rho_a U^2 B_2 B_5 B_1^{-1} B_2$ (aerodynamic stiffness)

$M = M_s + M_a$

$M_s = -\rho_s B_1$ (structural mass)

$M_a = 2\rho_a B_1 B_5$ (added air mass)

$D = \rho_a U B_1 (B_5 B_1^{-1} B_2 + B_1^{-1} B_2 B_5)$

(aerodynamic damping)

4. Stability criteria

Above Eq. (21) is a quadratic eigenvalue problem. We can change it into a general form by introducing $w^* = \lambda \overline{w}$, then

$$\begin{bmatrix} 0 & I \\ -M^{-1}K & -M^{-1}D \end{bmatrix} \begin{Bmatrix} \overline{w} \\ w^* \end{Bmatrix} - \lambda \begin{Bmatrix} \overline{w} \\ w^* \end{Bmatrix} = 0 \quad (22)$$

Assuming that system has n degrees of freedom, therefore, Eq. (22) has $2n$ eigenvalues and eigenvectors. We write it as $\Lambda = diag(\lambda_1, \lambda_2, \cdots, \lambda_{2n})$, and the corresponding eigenvectors are $X = [x_1, x_2, \cdots, x_{2n}]$. Thus, the displacement could be expressed based on these eigenvalues and eigenvectors.

$$\overline{w}(t) = \sum_{j=1}^{2n} a_j x_j e^{\lambda_j t} \quad (23)$$

Where, a_j - arbitrary constant coefficient

Generally, eigenvalues are complex values. $\lambda_j = \gamma_j + i\cdot\omega_j$, $i=\sqrt{-1}$. From Eq. (23), we can know that the system is stable only when all of the real parts of the eigenvalues are less than 0. As long as one is larger than 0, the system is unstable. Among them, if the real part is larger than 0 and the imaginary part is equal to 0, which will give rise to an exponentially growing motion without vibration. This kind of instability is called as "divergence". If the real parts is larger than 0 and the imaginary part is not equal to 0, then the instability could be called as "flutter". The occurrence of flutter requires the coalescence of two natural frequencies. The physical interpretation of the flutter phenomenon is that one vibration mode absorbs energy and feeds it into another.

Stability criteria as shown in Fig. 4 could be

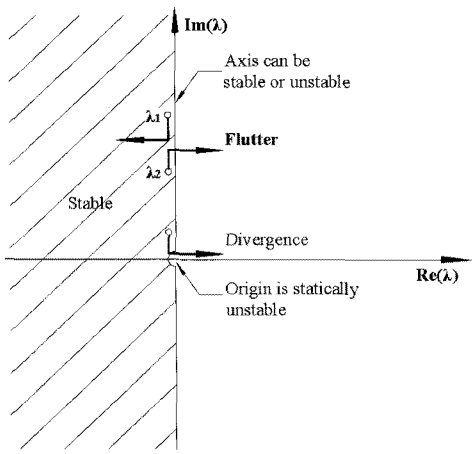

Fig. 4 stability criteria

summarized as follows.

(1) Divergence: $\mathrm{Re}(\lambda_j)>0$ and $\mathrm{Im}(\lambda_j)=0$ for any one of the eigenvalues.

(2) Flutter: $\mathrm{Re}(\lambda_j)>0$ and $\mathrm{Im}(\lambda_j)\neq 0$ for any one of the eigenvalues.

5. Numerical examples

5.1 square membrane structure

As shown in Fig. 5 and Fig. 6, 6m×6m Square membrane with four sides fixed, the density of membrane ρ_s is 1.05kg/m^2. The air density takes 1.21kg/m^3. Wind interacts with membrane on its upper surface with a constant velocity U. The air under the membrane is regarded as static(U=0).

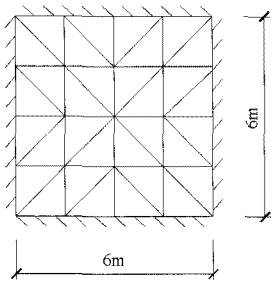

Fig. 5 Square membrane

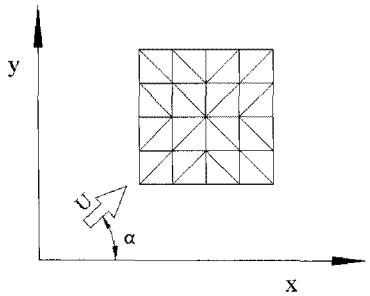

Fig. 6 Wind direction

5.1.1 Circular frequencies

Variation of circular frequencies with the increase of wind velocity is shown in Fig. 7. Here, prestressing forces in the x direction and y direction are same, and wind moves along the x direction of the membrane. When wind velocity approaches to about 45m/s, the 1st circular frequency decreases to 0. The membrane becomes instability of divergence type. When wind velocity is increased to 52m/s, the 2nd circular frequency also decreases to 0. When wind velocity reaches 55m/s, these two modes are combined together. With the increase of the combined circular frequency, membrane gets into instability region of flutter type.

As shown in Fig. 7, when the wind velocity is 0, the value of circular frequency is natural frequency.

5.1.2 Influence of prestressing force

The relationship between critical wind velocity and prestressing force is shown in Fig. 8. The lower line shows the critical wind velocity for divergence type instability U_{cd}, while the upper line shows the critical wind velocity for flutter type instability U_{cf}. At the same time, these two lines divide the total area into three parts. These three regions are stable region, divergence region and flutter region from the bottom up.

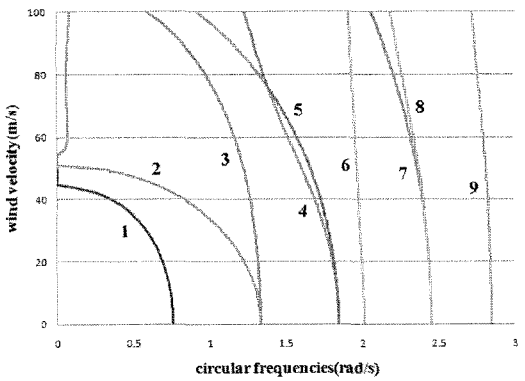

Fig. 7 Circular frequencies variation
(1, 2, ···, 9 are the number of eigenvalues)

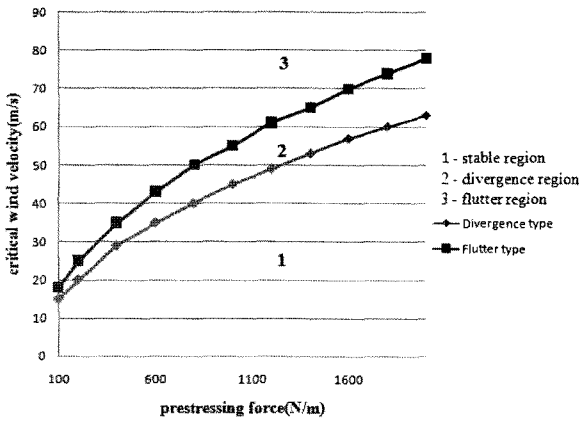

Fig. 8 Influence of prestressing force

Apart from that, we could obtain that the critical wind velocity increases with prestresing force, which is correct for both divergence type and flutter type instability. Therefore, the reasonable prestressing force could prevent the occurrence of instability.

5.1.3 Influencing of wind direction

When wind direction is not along the axis of membrane but with an angle ±, the relationship between critical velocity and wind direction are shown in Fig. 9. From Fig. α, the relationship between critical velocity and wind direction are shown in Fig. 9. From Fig. 9, we can obtain the relationship between critical velocity and wind direction. When angle α=45°, the critical velocity of divergence type reaches its maximum, while the critical velocity of flutter type reaches its minimum. Therefore, the most dangerous angles for divergence type instability are 0° and 90°. On the contrary, the most dangerous angle for flutter type is 45°.

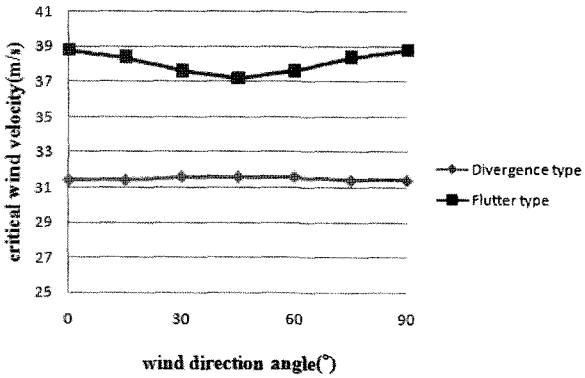

Fig. 9 Influence of wind direction($T_x = T_y = 500N/m$)

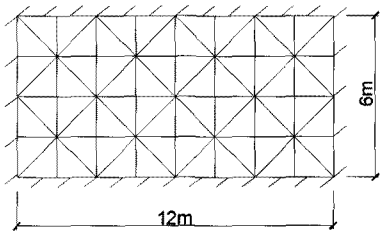

Fig. 10 Rectangular membrane

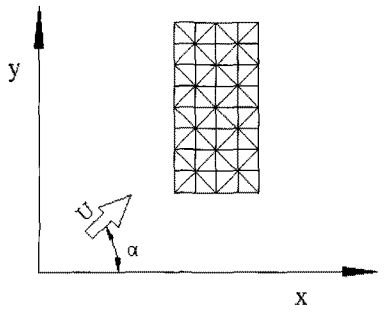

Fig. 11 Wind direction angle

5.2 Rectangular membrane structure

12m×6m rectangular membrane with four sides fixed is divided into 64 elements(as shown in Fig. 10). Structure has 21 degrees of freedom. Wind field condition and membrane material are same with above example. Wind direction angle is shown in Fig. 11.

5.2.1 Circular frequencies

Circular frequencies variation with the increase of wind velocity is shown in Fig. 12. These variations also depend on wind direction. Thus, we analyze two extreme situations: angle α are 0° and 90°.

As we know, flutter type instability happens when two modes are coupled. As shown in Fig. 12, when wind direction angle α is 0°, with the increase of wind velocity up to 32m/s, circular frequency of mode 1 decrease to 0, structure becomes instability of divergence type. When wind velocity continues increasing, circular frequency of mode 1 increases and converges with mode 4 at 35m/s, structure becomes instability of flutter type.

Different from the situation above, when angle α is 90°, circular frequency of mode 1 decreases to 0 at 32m/s. However, the real part of the eigenvalue is

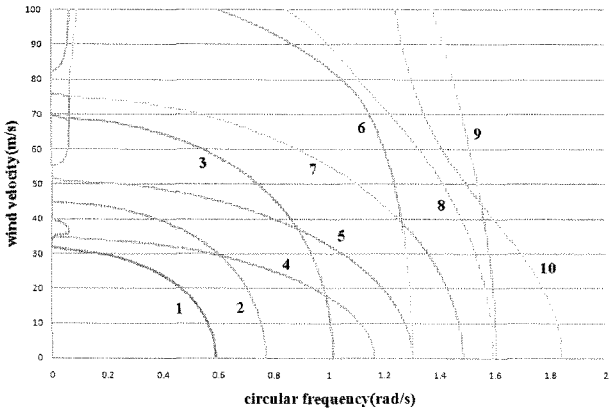

(a) $\alpha = 0°$ and $T_x = T_y = 1000N/m$

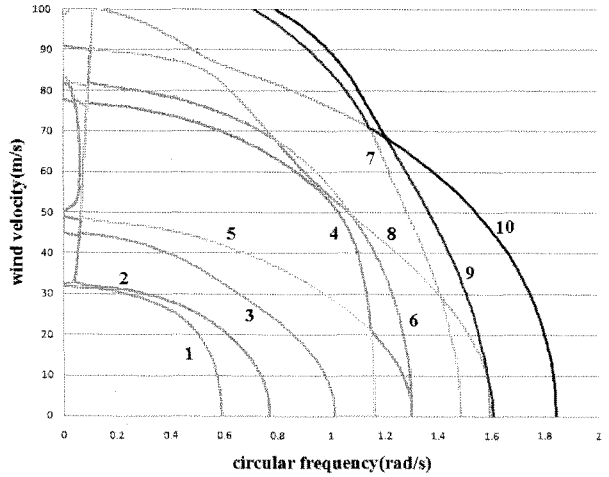

(b) $\alpha = 90°$ and $T_x = T_y = 1000N/m$

Fig. 12 Circular frequencies variation

negative at this time, so the structure is stable. When wind velocity increases to 33m/s, two modes converge at one point, structure becomes flutter type instability. Of course, there are also other converging points at higher wind velocities, but we are generally interested in the lowest wind velocity at which instability occurs, so we will not interpret it in detail.

5.2.2 Influence of prestressing force

The relationships between prestressing force and critical wind velocity are shown in Fig. 13. As introduced in 5.2.1, towards different wind direction, their instability forms are different. When wind direction angle α is 0°, structure becomes instability of divergence type before flutter type. However, when angle α is 90°, structure becomes flutter type instability firstly. Divergence occurs at a higher wind

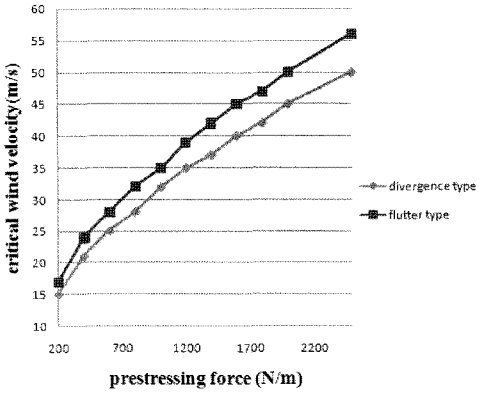

(a) $\alpha = 0°$

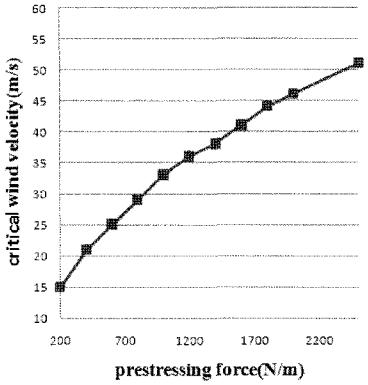

(b) $\alpha = 90°$

Fig. 13 Influential of prestressing force

velocity and its influential range is small, so we neglect it here.

6. Conclusion

In this paper, we take advantage of FEA method to study the aeroelastic instability of two-dimensional membrane structures. The basic principles and procedures are introduced in this paper. We could also obtain two important conclusions through numerical examples.

1. Prestressing force has a big impact on critical wind velocity, so we could select reasonable prestressing force to prevent the occurrence of instability.
2. Towards wind direction, its influence on critical wind velocity is very small for square membrane. However, it plays an important role in the occurrence of instability for rectangular membrane. Therefore, in order to avoid aeroelastic instability, optimal structure direction is also important.

Acknowledgements

This study is supported by the fund of Inha University(2009). We appreciate its help very much.

References

Bažant, Z. P., Luigi Cedolin (1991) Stability of structures (Elastic, Inelastic, Fracture and Damage Theories), Cambridge university press, New York.

Bisplinghoff, R. L., Ashley, H., Halfman, R. L. (1996) Aeroelasticity,Addison Wesley, Cambridge.

Brebbia, C. A., Telles, J. C. F., Wrobel, L. C. (1984) Boundary Element Techniques (theory and application in engineering), Springer-Verlag, Berlin.

Kornecki, A. (1976) On the aeroelastic instability of two-dimensional panels in uniform incompressible Flow, *Journal of Sound and Vibration*, 47(2), pp.163~178.

Kunieda, H. (1975) Flutter of hanging roofs and curved membrane roofs, International Journal of Solids and Structures, 11, pp.477~492.

Levy, R., Spillers, W. R. (1995) Analysis of Geometrically Nonlinear Structures, Chapman & Hall, New York.

Logan, D. L. (2002) A First Course in the Finite Element Method (Third edition), Brooks/Cole, California.

Lucey, A. D., Carpenter, P. W. (1993) The hydroelastic stability of three-dimensional dsturbances of a finite compliant wall, *Journal of Sound and Vibration*, 165(3), pp.527~552.

Newman, B. G., Paidoussis, M. P. (1991) The stability of two-dimensional membranes in streaming flow, *Journal of Fluids and Structures*, 5, pp.443~454.

Press, W. H., Teukolsky, S. A., Vetterling, W. T., Flannery, B. P. (1992) Numerical Recipes in Fortran (second edition), Cambridge university press, Cambridge.

Sygulski, R. (1993) Vibration of pneumatic structures interacting with air, *Computer & Structures*, 49(5), pp.867~876.

Sygulski, R. (1996) Dynamic stability of pneumatic structures in wind: theory and experiment, *Journal of Fluids and Structures*, 10, pp.945~963.

Sygulski, R. (1997) Numerical analysis of membrane stability in air flow, *Journal of Sound and Vibration*, 207(3), pp.281~292.

Sygulski, R. (2007) Stability of membrane in low subsonic flow, *International Journal of Non-linear Mechanics*, 42, pp.196~202

Zienkiewicz, O. C., Taylor, R. L., Zhu, J. Z. (2005) The Finite Element Method: Its Basis and Fundamentals(six edition), Butterworth-Heinemann, Oxford.